Ultrasonics Sonochemistry 90 (2022) 106168

Contents lists available at ScienceDirect

Ultrasonics Sonochemistry

journal homepage: www.elsevier.com/locate/ultson

Root canal irrigation system using remotely generated high-power ultrasound

Ryeol Park [a,1], Minsu Choi [a,1], Jaedeok Seo [a], Eun Hyun Park [b,*], Sung Wook Jang [c], Won-Jun Shon [b], Ho-Young Kim [d,*], Wonjung Kim [a,e,*]

[a] Department of Mechanical Engineering, Sogang University, Seoul 04107, Republic of Korea
[b] Department of Conservative Dentistry, Dental Research Institute and School of Dentistry, Seoul National University, Seoul 03080, Republic of Korea
[c] Maruchi Co., Ltd., Wonju 26311, Republic of Korea
[d] Department of Mechanical Engineering, Seoul National University, Seoul 08826, Republic of Korea
[e] Institute of Emergent Materials, Sogang University, Seoul 04107, Republic of Korea

ARTICLE INFO

Keywords:
Ultrasonic cleaning
Root canal irrigation
Root canal treatment

ABSTRACT

Root canal treatment is performed to remove the bacteria proliferating in the root canals of a tooth. Many conventional root canal irrigation methods use an instrument inserted into the root canals. However, bacteria removal is often incomplete in the apical region of the root canal, and the treatment carries clinical risks, such as instrument fracture and extrusion of irrigation liquid through the canal apex. We here suggest a novel, remotely generated high-intensity ultrasound irrigation system that exhibits better irrigation performance and a reduced clinical risk. Our device employs powerful ultrasonic waves generated by a transducer placed outside a target tooth. The generated ultrasonic waves are guided to travel into the root canals. In the root canals of the target tooth, acoustic cavitation occurs, and vapor bubbles are created. The dynamic motions of vapor bubbles create remarkable cleaning effects. Using root canal models, we tested the cleaning performance of the proposed system and compared it with other conventional irrigation methods. The results revealed that biofilm in the apical region of the root canal models can be removed exclusively using the proposed system, thus demonstrating an improvement in cleaning performance. We also measured pressure at the apex of the root canals of an extracted tooth while operating the proposed system. Our system exhibited a smaller pressure compared to the syringe irrigation method, thus suggesting a reduced risk of apical extrusion of the irrigation liquid. Since the proposed system operates without inserting instruments into the root canal, it can clean multiple root canals in a tooth simultaneously with a single treatment. The proposed device would be a breakthrough in root canal treatment in terms of irrigation performance, clinical safety, and ease of treatment.

1. Introduction

A root canal is an anatomic space in a tooth filled with soft tissue containing nerves and blood vessels. An individual root canal typically has a narrow, long channel shape, and root canals can be connected with lateral canals, isthmus, and apical ramification to form a network [1,2]. When bacteria in an oral cavity penetrate to a root canal network, they can proliferate and cause severe inflammation and pain [3]. The root canal treatment, so-called endodontic treatment, is a clinical procedure of removing the proliferated bacteria and occluding the canals with inert fillers [1,4]. The treatment process can be divided into several steps: opening the pulp chamber, cleaning the root canals, and obturating the root canals [2,5,6]. Root canal cleaning is a crucial step for successful treatment since remnant bacteria inside the root canals can lead to reinfection [7,8].

Various root canal cleaning methods are available (see Fig. 1). Syringe irrigation (SI), one of the most conventional methods, refers to injecting irrigation liquid through a syringe needle that is inserted into

* Corresponding authors at: Department of Conservative Dentistry, Dental Research Institute and School of Dentistry, Seoul National University, Seoul 03080, Republic of Korea (E.H. Park); Department of Mechanical Engineering, Seoul National University, Seoul 08826, Republic of Korea (H.-Y. Kim); Department of Mechanical Engineering, Sogang University, Seoul 04107, Republic of Korea (W. Kim).
E-mail addresses: eunh.park@gmail.com (E.H. Park), hyk@snu.ac.kr (H.-Y. Kim), wonjungkim@sogang.ac.kr (W. Kim).
[1] Both authors equally contributed to this work.

https://doi.org/10.1016/j.ultsonch.2022.106168
Received 30 June 2022; Received in revised form 27 August 2022; Accepted 15 September 2022
Available online 15 September 2022

the root canal [9]. The physical mechanism of SI was investigated using computational fluid dynamics in some previous studies [10–12]. The studies presented the velocity and pressure fields induced by the irrigant injection at the needle, suggesting that SI is effective near the needle tip. However, the needle can be inserted to a limited depth in the root canal, thus often resulting in incomplete cleaning in the apical region [13]. In addition, SI carries a clinical risk of extruding the irrigant through the root canal apex, as supported by the previous computational simulations [10,11]. Extrusion of the irrigant through the root canal apex can lead to hemolysis, ulcers, and tissue necrosis with serious pain [14–16]. Although a great deal of effort has been devoted to reducing the clinical risks of apical extrusion by developing various needles, such as side-vented closed-end needles (see the inset of Fig. 1a), SI still carries the risk of apical extrusion of irrigation liquid [17].

Root canal cleaning methods using a file with high-frequency vibration are also widely used [18]. Passive sonic irrigation (PSI) employs a polymer tip that vibrates to agitate the irrigation liquid in a root canal (see Fig. 1b) [18–20]. Passive ultrasonic irrigation (PUI) refers to an irrigation method that uses a high-frequency vibrating metal tip that generates cavitation around the tip, which creates a cleaning effect in the root canal (see Fig. 1c) [21]. Substantial efforts have been devoted to understanding the hydrodynamics associated with PSI and PUI, demonstrating that irrigant streaming and cavitation induced by vibrating tips primarily lead to root canal cleaning [22–27]. However, PSI and PUI can also result in insufficient cleaning. Vibrating tips can easily contact the inner wall of the root canal, and this contact limits the tip vibration and thus markedly mitigates the acoustic energy delivered to the irrigant [23,28]. There is a risk of apical extrusion as in SI because both methods require a final step of flushing with a syringe needle. Moreover, PUI uses a brittle metal tip with dynamic motion and thus carries an additional clinical risk of tip fracture in the root canal, which may require surgical retreatment [19,29].

Laser activated irrigation (LAI) has been developed relatively recently to improve irrigation performance [30,31]. LAI uses a pulsed laser to create cavitation bubbles, and the dynamic motion of cavitation bubbles induce a cleaning effect in root canals [30–32]. LAI can be advantageous because they can be used without the insertion of instruments into the root canals. Clinical systems using LAI are commercially available, but LAI is currently less popular than other methods.

Ultrasonic cleaning has been used in various engineering fields, such as semiconductor manufacturing [33–36], and the mechanisms have been extensively investigated. In an ultrasonic field with sufficient acoustic pressure, cavitation bubbles can be generated by stretching of the liquid during the rarefaction phase of sound waves [37,38]. A cavitation bubble will exhibit dynamic motion in response to the acoustic waves, and this induces microscale flows around the bubble, including vortical flows and high-speed jets, which are responsible for the ultrasonic cleaning effect [39–42].

Here, we propose a novel, remotely generated high-intensity ultrasound irrigation system (RS) for root canal treatment. RS employs powerful ultrasonic waves generated by a transducer placed outside the tooth during treatment. The generated ultrasonic waves are guided to travel into the root canals. Acoustic cavitation occurs in the root canals of a target tooth, and vapor bubbles are created. The dynamic motions of the vapor bubbles produce remarkable cleaning effects. Using engineered root canal models, we conducted tests to assess the cleaning performance of the proposed system and compared the results to other existing methods, SI, PSI, and PUI. The results revealed that only RS completely cleaned the apical region of the root canal model. We also examined the apical pressure to quantify the risk for apical extrusion of irrigation liquid during treatment. The pressures measured for RS were lower than those measured for SI, thus suggesting better clinical safety with RS. Since RS operates without having to insert instruments into root canals, it can clean multiple root canals in a tooth simultaneously with a single treatment. The innovative design of RS, which employs high-power ultrasound excited by a large ultrasonic transducer outside the target tooth in combination with an acoustic reflector, is expected to be a breakthrough in root canal treatment in terms of irrigation performance, clinical safety, and ease of treatment.

2. Materials and methods

2.1. Design and operation of RS

Fig. 2 displays the RS design. The system is composed of a 40 kHz piezoelectric ultrasonic transducer connected to a cylindrical horn. The horn and transducer are enclosed by a housing structure. The housing was made of a photocurable resin using a stereolithography apparatus 3D printer (Form 3, Formlabs). The gap between the inner surface of the housing and the cylindrical horn was approximately 2 mm. The housing was connected to a 3 mm diameter tube to allow the inflow of cooling water and had an outlet in the form of a 6 mm diameter circular opening. An acoustic reflector was built on the distal part of the housing. A 1-mm-thick stainless-steel plate in an elliptical shape with a major axis length of 17 mm and a minor axis length of 10 mm was placed at a location 5 mm away from the horn tip at an angle of 45°. The density of the stainless-steel plate used in the system is approximately 7,500 kg/m^3, and the sound speed through the stainless-steel is approximately 6,000 m/s. The irrigant injection nozzle was located in the lower part of the housing. The inner diameter and total length of the nozzle were approximately 150 μm and 10 mm, respectively, and the nozzle tip was bent 90° so that the irrigation liquid is injected into the pulp cavity of a target tooth.

During the operation of the system, a peristaltic pump (KFS-HA1B10Y, Kamoer) supplies degassed cooling water to the housing at a

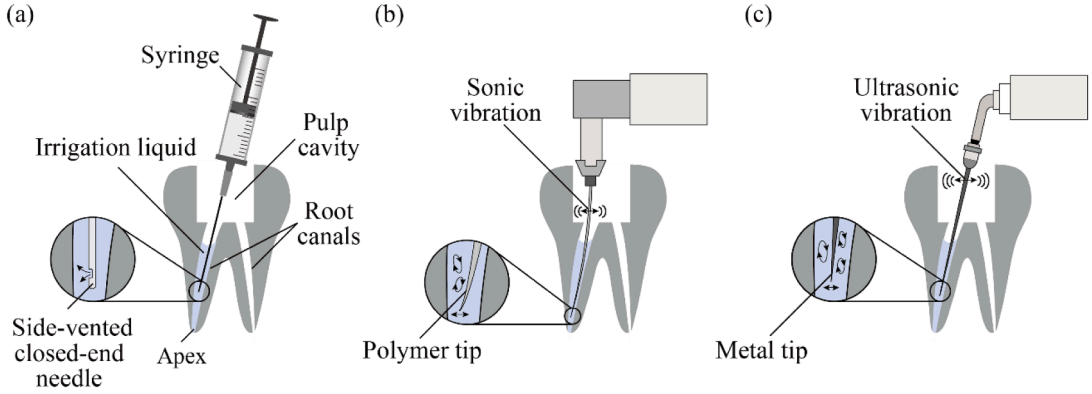

Fig. 1. Schematics of (a) syringe irrigation, (b) passive sonic irrigation, and (c) passive ultrasonic irrigation.

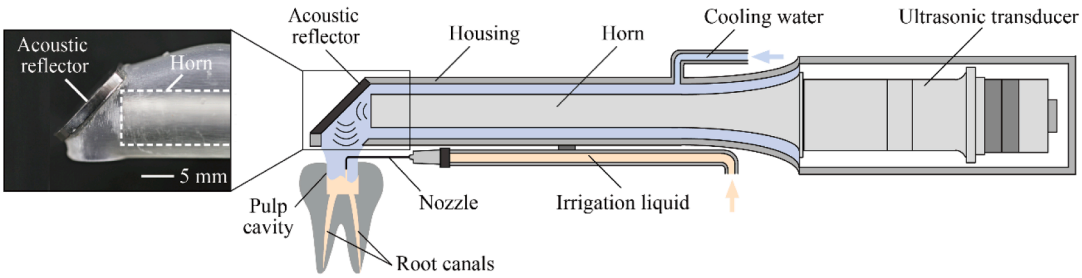

Fig. 2. Schematic of the remotely generated high-intensity ultrasound irrigation system (RS).

volumetric flow rate of 30 mL/min. Water flows through the gap between the horn and inner wall of the housing and leaves the housing through the outlet. The water carries heat from the transducer and horn during the operation. Water occupying the interior space of the housing mediates the transmission of ultrasonic waves from the horn to the housing outlet. When electric power is applied to the ultrasonic transducer, a longitudinal vibration is produced and transmitted through the horn. The intensity of longitudinal vibration is enhanced in the horn because the diameter of the horn is 8 mm, which is smaller than the transducer diameter of 30 mm [43]. The acoustic reflector changes the propagation direction of the ultrasonic waves emitted from the horn tip, so that the ultrasonic waves are propagated in the direction of the outlet of the housing. We measured the acoustic pressure of the reflected waves at the housing outlet. A hydrophone (TC4038, Teledyne RESON) was submerged in a bath filled with degassed water, and the housing outlet was placed 1 mm above the hydrophone while the housing was partially submerged. The acoustic pressure was measured to be 180–250 kPa. Degassed irrigation liquid was supplied by a liquid pump (CNB1-02, CNHT) through the passage below the housing at a flow rate of 20 mL/min.

2.2. Ultrasound reflection on the acoustic reflector

To examine the reflection of ultrasonic waves on the acoustic reflector, we conducted cleaning test using the experimental setup shown in Fig. 3. The ultrasonic horn combined with the transducer without the housing was held on a support in a bath that was 90 mm, 90 mm, 70 mm in width, depth, and height, respectively. A stainless-steel plate similar to the one used as the acoustic reflector was placed 8 mm below the horn tip, and a glass substrate was placed 12 mm from the reflection plate. The glass substrate was contaminated with 4 μm diameter polystyrene particles (C37253, Life technologies). To control their adhesion force, after the particles were sprayed on the glass substrate, it was baked on a hot plate at a temperature of 125 °C for 5 min [38]. Since some clustered particles remained weakly adhered to the substrate, the contaminated glass substrate was gently rinsed with water before the cleaning test [38,44]. After filling the bath with degassed water, we operated the transducer for 6 min. We quantified the result of cleaning of the contaminated substrate with and without the acoustic reflector in terms of particle removal efficiency (PRE), defined as $\eta = (C_0 - C)/C_0$ with C_0 and C being the number of particles deposited on the substrates before and after cleaning, respectively. The number of particles was estimated by measuring the surface area covered with particles of the substrate. We also measured the acoustic pressure at the same location as the contaminated substrate using a hydrophone (TC4038, Teledyne RESON) with and without the acoustic reflector.

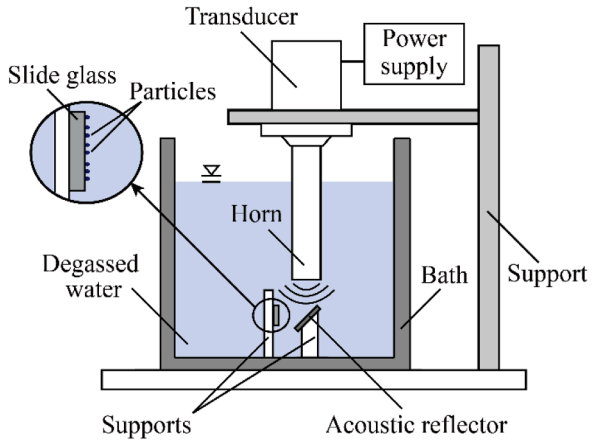

Fig. 3. Experimental setup to test the reflection of ultrasonic waves on the acoustic reflector.

2.3. Visualization of cavitation bubbles generated by RS

We visualized cavitation bubbles generated by RS using a setup shown in Fig. 4. A glass cylinder with an inner diameter of 4 mm was placed below the outlet of the housing. The motion of cavitation bubbles at 2 mm below the housing outlet was recorded using a high-speed camera (Fastcam Mini AX200, Photron) combined with a long-distance microscope lens (12X Zoom, Navitar). A light source was placed on the opposite side of the high-speed camera.

2.4. RS cleaning performance

Two engineered root canal models were used to test the cleaning performance of the RS. Fig. 5a shows the root canal model, which had a single canal. This model had a tapering channel with a curvature of 30°, measured using the Schneider method [45]. The length of the channel and the diameter of the channel inlet were measured to be 11 mm and 400 μm, respectively, and an apical foramen had a diameter of 200 μm. Fig. 5b shows the other root canal model fabricated using a 3D printer (SLA 600, Protofab) with transparent resin. This model had three straight channels and two curved channels, and the diameter of all the apical foramens was approximately 400 μm.

To simulate a thin microbe and bacteria biofilm proliferated in the

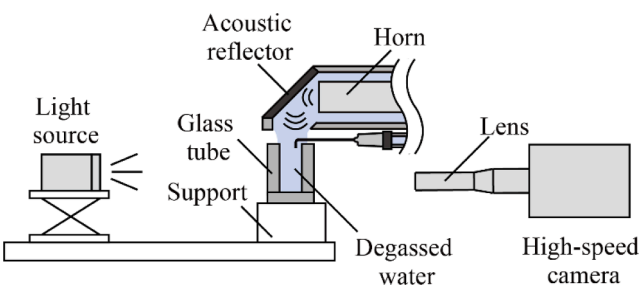

Fig. 4. Experimental setup to visualize cavitation bubbles.

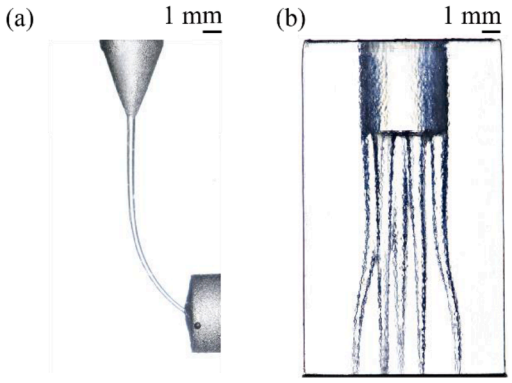

Fig. 5. The root canal models with (a) a single curved root canal and (b) multiple root canals.

root canal [46–48], we filled the channels with a calcium hydroxide-based paste (Calcipex II, Nishika) and left the paste only near the root canal wall using a dental file. Contaminated canals appeared black due to the opaque paste film adhering to the root canal wall. All the apical foramens of the models were completely sealed with a polyvinyl siloxane impression material (Blu-mousse, Parkell Bio-Materials) before cleaning.

The contaminated root canal models were cleaned using RS for 6 min. For comparison, we also cleaned the contaminated models using the SI, PSI, and PUI methods. To test SI, a 30-gauge side-vented closed-end needle was inserted to a depth approximately 4 mm from the inlet, and water was injected at a flow rate of 3 mL/min for 2 min. For the test with PSI, an Endoactivator (EA) (Dentsply Tulsa Dental Specialties) was combined with a flexible vibrating tip (#20/0.02, Dentsply Tulsa Dental Specialties). To test the PUI, an ultrasonic unit (Suprasson P5 Booster, Satelec Acteon) combined with an irrisafe tip (#20/0.00, Satelec Acteon) was used. In the tests for PSI and PUI, a single process consisting of 30 s of tip vibration and 10 s of needle flushing with a 30-gauge side-vented closed-end needle was repeated three times. Each irrigation method of PSI, PUI, and RS was repeated three times to confirm the reproducibility of cleaning performance. Although chemical solutions such as NaOCl (2.5 wt%) are commonly used in clinical treatments, water was used as the irrigation liquid to remove the chemical effects from the irrigation methods and to reveal only the mechanical effects. The root canal models were observed using a DSLR camera (EOS 70D, Canon) with a macro lens (RF 100 mm f/2.8, Canon) before and after the cleaning process.

2.5. Measurement of apical pressure

Fig. 6 shows the experimental setup used for measuring pressure at the apex of the root canals. A root canal of a human tooth with multiple root canals was shaped using a Ni-Ti rotary file (#20/0.04, Dentsply Maillefer) combined with an endomotor (X-Smart plus, Dentsply Maillefer) to have an apical diameter of 200 μm. The apex of the shaped canal was kept open, and the other apexes were sealed with the polyvinyl siloxane impression material (Blu-mousse, Parkell Bio-Materials). The tooth was fixed in a closed chamber equipped with a pressure sensor (PX409-2.5CGUSBH, Omega), and the chamber and inner space of the tooth were filled with water. We measured the pressures during the operation of the RS. For comparison, we also measured the apical pressure during the operation of SI, in which a 30-gauge side-vented closed-end needle was placed at a distance 3 mm away from the apical foramen, and water was injected at a flow rate of 3 mL/min for 1 min. We measured the average apical pressure in three repeated tests. The study was approved Institutional Review Board of Seoul National University Dental Hospital, Seoul, Korea (IRB No. CRI22004).

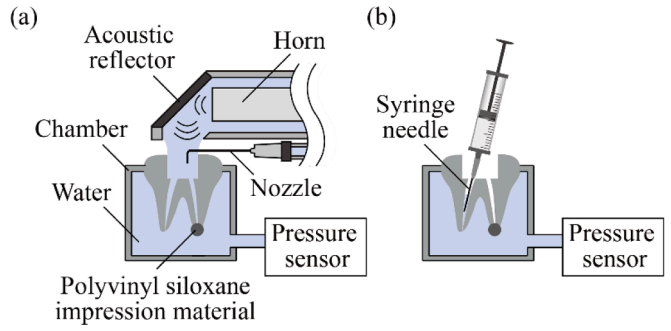

Fig. 6. Experimental setup used to measure apical pressure produced by (a) RS and (b) SI.

3. Results and discussion

3.1. Ultrasound reflection on the acoustic reflector

The RS employs a large transducer connected with a lengthy horn, which cannot be accommodated in the direction normal to the pulp cavity of a tooth in a clinical process. Since ultrasound mainly propagates longitudinally, a change in the direction of propagation is required. The acoustic reflector in RS has been designed to guide ultrasonic waves to travel from the horn to the root canals by changing the propagation direction of the ultrasonic waves. When propagating acoustic waves meet an interface of two media at an angle, they are reflected on the interface at the same angle [49]. In RS, the acoustic reflector is placed to meet the incident acoustic waves at 45°, so the incident waves are reflected in the direction of the tooth chamber.

The ratio between the acoustic pressures of the incident and reflected waves is expressed as $(Z_2 - Z_1)/(Z_2 + Z_1)$, where $Z = \rho c$ with ρ being the density of the medium and c being the sound speed [50], and the subscripts 1 and 2 denote the medium in which the incident and absorbed ultrasonic waves propagate, respectively [49]. In a case where Z_2 is much greater than Z_1, $(Z_2 - Z_1)/(Z_2 + Z_1)$ is approximately 1, suggesting that acoustic waves are reflected with little absorption at the interface of the two materials. The acoustic reflector in the RS is made of stainless steel with $Z_2 = 45$ kg/mm^2·s, which is much greater than that of water, $Z_1 = 1.5$ kg/mm^2·s, so approximately 90 % of the incident acoustic waves are expected to be reflected by the acoustic reflector.

We measured acoustic pressure with and without the acoustic reflector using the setup shown in Fig. 3. While the acoustic pressure with the acoustic reflector was measured to be approximately 220 kPa, it was significantly reduced to 80 kPa without the acoustic reflector, as shown in Fig. 7a. Such a notable difference in the acoustic pressure results in a difference in cleaning efficiency. We measured the PRE to be approximately 98 % with the acoustic reflector and less than 20 % without the acoustic reflector (see Fig. 7b). The result therefore demonstrates that the acoustic reflector guides ultrasound waves to travel to the contaminated substrate by changing the transmitted direction of the ultrasound waves.

3.2. Characteristics of cavitation bubbles generated by RS

Although the content of cavitation bubbles is typically a mixture of gas and vapor, cavitation bubbles can be classified as either gas or vapor bubbles depending on the relative composition of the gas and vapor [38,51]. Cavitation bubbles produced in degassed liquids are often referred to as vapor bubbles [49,52], otherwise gas bubbles [49,53]. Because vapor can rapidly turn into liquid, vapor bubbles generally exhibit large oscillating amplitude and exist only for short periods. In contrast, once gas bubbles are formed, gas cannot diffuse into the liquid on the time scale of bubble oscillation. As a result, gas bubbles show small oscillating amplitude and survive much longer, often until they

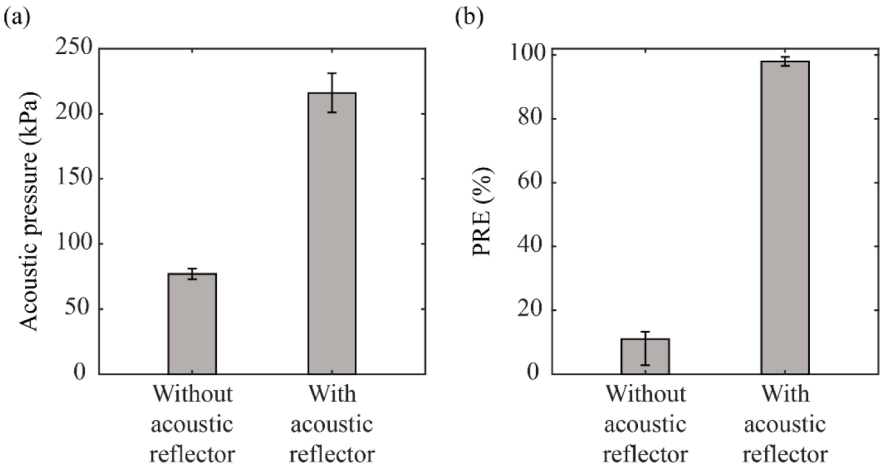

Fig. 7. Comparison of (a) acoustic pressures and (b) PREs with and without the acoustic reflector.

come out of the liquid [38].

Fig. 8 shows the bubbles generated by RS. As shown in Fig. 8a, numerous bubbles simultaneously appeared and disappeared in the field of view. We observed that most of the bubbles survived for less than approximately 10 ms, and the appearance of bubbles was continuously repeated during the operation of RS. In Fig. 8b, the oscillating motion of the bubbles was clearly observed in a single period of acoustic wave from 0 to 25 μs. Specifically, the bubbles were momentarily invisible during the contraction phase at 12.5 μs, indicating a large oscillation amplitude. Our experimental observations thus suggest that cavitation bubbles generated by RS were vapor bubbles rather than gas bubbles.

The gas content dissolved in the liquid can serve as seeds for the cavitation inception, so cavitation in ordinary, non-degassed liquids occurs at a relatively low acoustic pressure [38,54]. However, due to the gas cushioning effect, gas bubbles produce cleaning effects only in their vicinity while translating around on the solid substrate [38,39]. In contrast, creating vapor cavitation bubbles requires a relatively high acoustic pressure, but vapor bubbles show much more vigorous dynamic motion, including collapse with a high-speed liquid jet near a solid boundary, leading to a powerful cleaning effect [38,55]. By employing a large ultrasonic transducer capable of generating vapor cavitation bubbles, RS was designed to create a powerful cleaning effect in root canals.

3.3. Cleaning performance

Fig. 9 shows the results of cleaning the 11 mm-long single channel root canal model using the RS and other devices. Since the channel contaminated with a calcium hydroxide-based paste (Calcipex II, Nishika) is opaque, the cleaned part appeared transparent. Because cleaning started at the entrance of the model root canal and progressed to the apex, we quantified the cleaning performance using the length of the transparent part of the channel measured from the opening. By measuring the brightness of the images before and after irrigation, it was assumed that cleaning was completed to the depth where the local brightness was reduced. This method could overestimate the cleaning effect of PSI and PUI for which the boundary of the cleaned region was unclear (see Fig. 9c-d), but the length of the obscure region was less than approximately 1 mm. Using the SI, PSI, and PUI methods, the average lengths of the cleaned part in three repeated tests were 3 mm, 4 mm, and 7 mm, respectively, indicating that only the upper part of the channel was cleaned, and there was little cleaning effect in the apical region. In contrast, the RS resulted in complete cleaning of the apical region in three repeated tests, as evidenced by the fact that the entire length of the channel, 11 mm, became transparent.

Since the apex of the root canal was completely sealed to simulate periradicular tissue in our experiments, contaminants had to be removed through the channel inlet, which naturally made cleaning of the apical region difficult. When using devices with an instrument that is inserted into the channel, cleaning tends to be effective, primarily in the region close to the tip of the instrument [21,56,57]. For narrow, curved root canals, such as the channel used in our experiment, it is challenging to insert an instrument into the root canal to a sufficient depth. Even in the case where a vibrating instrument can be inserted to the apical region,

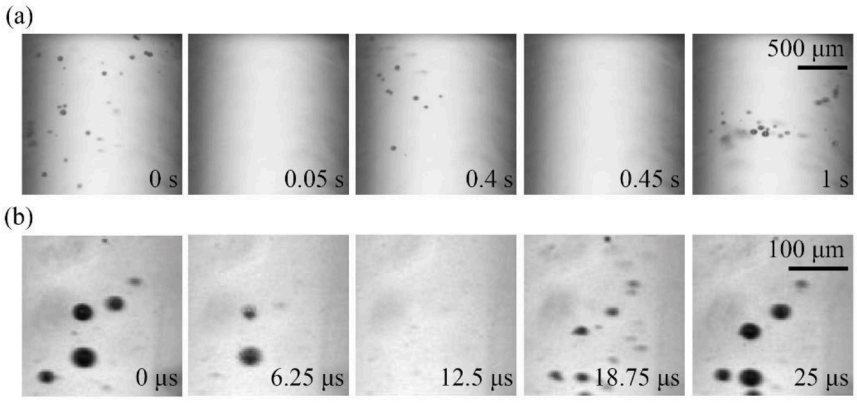

Fig. 8. Sequential images of cavitation bubbles generated by RS.

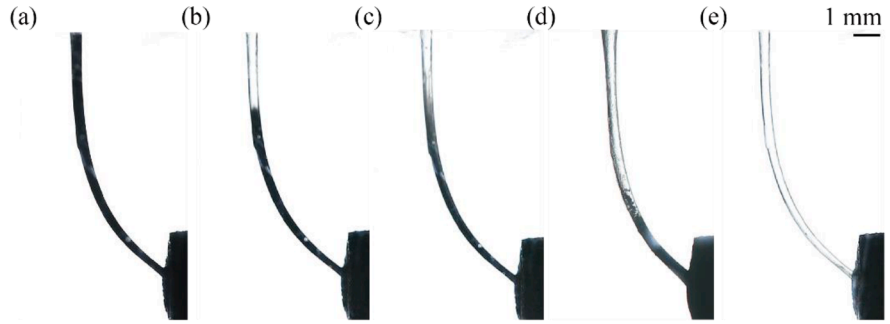

Fig. 9. The cleaning results for the root canal model with a single channel. The images represent (a) the contaminated channel before cleaning and the channels after cleaning with (b) SI, (c) PSI, (d) PUI, and (e) RS.

the file oscillation can be considerably hampered because of file-to-wall contacts. [23,28]. To overcome this limit, root canals can be enlarged significantly [58], but irrigation with minimal root canal enlargement is advantageous, to preserve natural tissue and tooth structure [59,60] and prevent apical extrusion [61]. The RS produces a cleaning effect by delivering strong ultrasound generated by a powerful horn-type transducer located outside the pulp cavity through a narrow and curved channel, providing advantageous for minimally invasive treatment.

Fig. 10 shows the results of cleaning tests using a root canal model with multiple channels. The results indicate that RS enables five root canals to be cleaned concurrently and thoroughly to the apical region in a single procedure. Unlike SI and PUI, which require repeated processes to insert the instrument into individual root canals, the RS can be used without skilled technique for instrument insertion and can save operating labor during treatment.

3.4. Risk assessment of extrusion of irrigation liquid through tooth apexes

One of the primary risks associated with root canal treatment is the extrusion of irrigation liquid out of the tooth apexes. Fig. 11 presents measurement of the pressure at the apical region during RS operation. While the apical pressure for SI was approximately 2 kPa, RS exhibited 0.5 kPa, much less than that of SI. The measured apical pressures of RS are comparable to those reported in the process of advanced root canal irrigation systems using pulsed lasers [32]. Although there is no available consensus for apical pressure to predict apical extrusion, some studies have reported that the apical pressure should remain below approximately 2 kPa to preclude apical extrusion [62,63]. Therefore, RS is not only safe to use, but can significantly lower the risk of apical extrusion compared to SI.

To understand the causes of apical pressures measured for RS, we also measured the pressures which occurred during operation just with ultrasound alone, and with irrigant jet only. The results shown in Fig. 11 reveal that without the irrigant jet the apical pressure remained insignificant, which suggests that the irrigant jet coming out of the nozzle is the primary cause of the apical pressure. We thus conjecture that acoustic waves or cavitation bubbles arising from the operation of the RS will have a negligible effect on apical pressure. The flow speed of the irrigation liquid in our device was controlled to be 20 m/s, which is higher than that of SI [9,64]. However, the nozzle was located in the pulp chamber, not in the root canal, and the irrgant jet had weaker effect on the apical pressure.

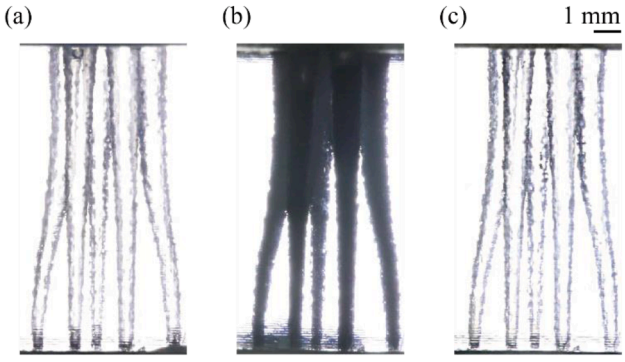

Fig. 10. The cleaning of the root canal model with multiple channels. The images represent the model (a) before contamination, (b) after contamination, (c) after cleaning with RS.

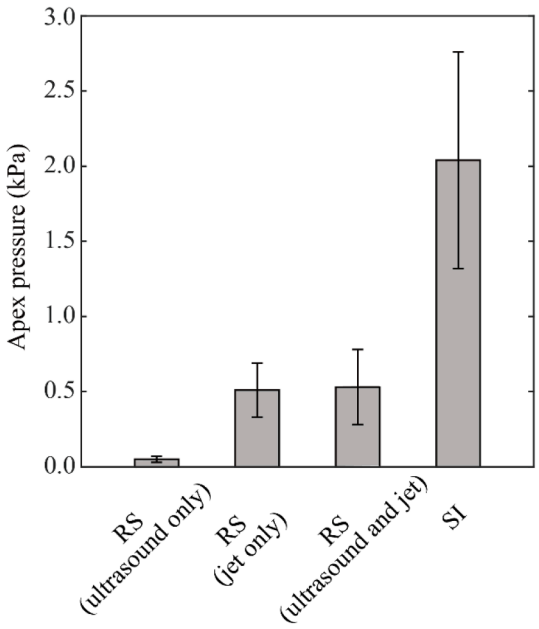

Fig. 11. Measurement of apical pressures during operation of the RS and SI. The error bars represent the range of measurements of instantaneous pressure.

The cavitation bubbles induced by the ultrasound are mainly responsible for removing the biofilm in the root canal, but they make an insignificant contribution to the apical pressure. In an attempt to improve the cleaning effect during irrigation using SI, a needle may be inserted into a deeper region or the flow rate may be increased. However, these techniques are highly limited due to the risk of apical extrusion of the irrigant [65,66]. Other instrument-insertion type irrigation protocols, such as PSI and PUI, may exhibit similar trade-offs between cleaning efficacy and clinical safety. It is because cleaning requires having sufficient access to the apical region, which however causes clinical risks, such as tip fracture in the root canal as well as the

apical extrusion of irrgant liquids. In contrast, cleaning effect and clinical risk are independent in RS because the cleaning action of the vapor cavitation bubbles has little negative effect on the apical pressure. This enables us to envision further improvements of the present novel but still early RS design, for example, by increasing the acoustic power.

Lastly, it is noteworthy that the key feature of our root canal irrigation system was achieved by using an acoustic reflector to deliver ultrasonic waves into a small, inaccessible space. Although the present study is focused on the clinical applications of ultrasound for dental treatment, the same technique could be used in other engineering fields, where there is a need to clean contaminated surfaces that are not directly accessible to ultrasonic transducers. For instance, conventional ultrasonic cleaning methods cannot be readily available for large-scale mechanical devices that are difficult to submerge in ultrasonic cleaning baths [67,68]. However, the technique proposed in the present study can be effective in cleaning the target contamination of such mechanical devices with minimal disassembly.

4. Conclusions

We have proposed a novel root canal irrigation system using remotely generated high-intensity ultrasound. The RS produces powerful ultrasonic waves, which are guided into the root canals of a tooth. Acoustic cavitation occurs in the root canal, and vapor bubbles produce the cleaning action in the root canal. Using simulated root canal models, we conducted cleaning tests which confirmed that RS was superior to other conventional root canal treatments using SI, PSI, and PUI for cleaning the apical region. RS exhibited lower apical pressure during operation than SI, thus suggesting better clinical safety. Our study demonstrated that RS has improved cleaning performance and better clinical safety compared to conventional root canal cleaning methods, so RS is expected to be a breakthrough in root canal treatment in terms of irrigation performance, clinical safety, and ease of treatment.

CRediT authorship contribution statement

Ryeol Park: Investigation, Writing – original draft. **Minsu Choi:** Investigation, Writing – original draft. **Jaedeok Seo:** Investigation, Validation. **Eun Hyun Park:** Investigation, Writing – review & editing. **Sung Wook Jang:** Conceptualization, Validation, Funding acquisition. **Won-Jun Shon:** Conceptualization, Writing – review & editing, Funding acquisition. **Ho-Young Kim:** Conceptualization, Writing – review & editing. **Wonjung Kim:** Conceptualization, Writing – original draft, Funding acquisition, Supervision.

Declaration of Competing Interest

The authors declare the following financial interests/personal relationships which may be considered as potential competing interests: R. Park, M. Choi, J. Seo, W.-J. Shon, H.-Y. Kim, and W. Kim have patent pending to Sogang University and Seoul National University.

Data availability

Data will be made available on request.

Acknowledgements

This work was supported by a grant of the Korea Health Industry Development Institute (KHIDI) funded by the Ministry of Health & Welfare (grant no. HI18C0432).

References

[1] F.J. Vertucci, Root canal anatomy of the human permanent teeth, Oral Surg. Oral Med. Oral Pathol. 58 (1984) 589–599.
[2] D. Ørstavik, V. Qvist, K. Stoltze, A multivariate analysis of the outcome of endodontic treatment, Eur. J. Oral Sci. 112 (2004) 224–230.
[3] B.P.F.A. Gomes, J.D. Lilley, D.B. Drucker, Clinical significance of dental root canal microflora, J. Dent. 24 (1996) 47–55.
[4] M.K. Çalişkan, Y. Pehlivan, F. Sepetçioğlu, M. Türkün, S.Ş. Tuncer, Root canal morphology of human permanent teeth in a Turkish population, J. Endod. 21 (1995) 200–204.
[5] A. Lussi, L. Messerli, P. Hotz, J. Grosrey, A new non-instrumental technique for cleaning and filling root canals, Int. Endod. J. 28 (1995) 1–6.
[6] J.M. Whitworth, N.H. Wilson, Rational root canal treatment in practice, Quintessence Publishing (2002).
[7] U. Sjögren, D. Figdor, S. Persson, G. Sundqvist, Influence of infection at the time of root filling on the outcome of endodontic treatment of teeth with apical periodontitis, Int. Endod. J. 30 (1997) 297–306.
[8] M. Zehnder, Root canal irrigants, J. Endod. 32 (2006) 389–398.
[9] Y. Shen, Y. Gao, W. Qian, N.D. Ruse, X. Zhou, H. Wu, M. Haapasalo, Three-dimensional numeric simulation of root canal irrigant flow with different irrigation needles, J. Endod. 36 (2010) 884–889.
[10] C. Boutsioukis, B. Verhaagen, M. Versluis, E. Kastrinakis, P.R. Wesselink, L.W. M. Van der Sluis, Evaluation of irrigant flow in the root canal using different needle types by an unsteady computational Fluid Dynamics model, J. Endod. 36 (2010) 875–879.
[11] C. Boutsioukis, C. Gogos, B. Verhaagen, M. Versluis, E. Kastrinakis, L.W.M. Van der Sluis, The effect of root canal taper on the irrigant flow: evaluation using an unsteady Computational Fluid Dynamics model, Int. Endod. J. 43 (2010) 909–916.
[12] B. Verhaagen, C. Boutsioukis, G.L. Heijnen, L.W.M. Van der Sluis, M. Versluis, Role of the confinement of a root canal on jet impingement during endodontic irrigation, Exp. Fluids 53 (2012) 1841–1853.
[13] L.S. Gu, J.R. Kim, J. Ling, K.K. Choi, D.H. Pashley, F.R. Tay, Review of contemporary irrigant agitation techniques and devices, J. Endod. 35 (2009) 791–804.
[14] P. Desai, V. Himel, Comparative safety of various intracanal irrigation systems, J. Endod. 35 (2009) 545–549.
[15] R.P. Mitchell, J.C. Baumgartner, C.M. Sedgley, Apical extrusion of sodium hypochlorite using different root canal irrigation systems, J. Endod. 37 (2011) 1677–1681.
[16] B. Basrani, M. Haapasalo, Update on endodontic irrigating solutions, Endod. Topics 27 (2012) 74–102.
[17] A. Alkahtani, T.D. Al Khudhairi, S. Anil, A comparative study of the debridement efficacy and apical extrusion of dynamic and passive root canal irrigation systems, BMC Oral Health 14 (2014) 1–7.
[18] K. Gulabivala, Y.L. Ng, M. Gilbertson, I. Eames, The fluid mechanics of root canal irrigation, Physiol. Meas. 31 (2010) R49.
[19] M. Kucher, M. Dannemann, N. Modler, C. Hannig, M.T. Weber, Effects of endodontic irrigants on material and surface properties of biocompatible thermoplastics, Dent. J. 7 (2019) 26.
[20] D. Donnermeyer, H. Wyrsch, S. Bürklein, E. Schäfer, Removal of calcium hydroxide from artificial grooves in straight root canals: sonic activation using EDDY versus passive ultrasonic irrigation and XPendo Finisher, J. Endod. 45 (2019) 322–326.
[21] R.G. Macedo, B. Verhaagen, D.F. Rivas, J.G. Gardeniers, L.W.M. Van der Sluis, P. R. Wesselink, M. Versluis, Sonochemical and high-speed optical characterization of cavitation generated by an ultrasonically oscillating dental file in root canal models, Ultrason. Sonochem. 21 (2014) 324–335.
[22] P.J. Lumley, A.D. Walmsley, W.R.E. Laird, An investigation into cavitational activity occurring in endosonic instrumentation, J. Dent. 16 (1988) 120–122.
[23] A.D. Walmsley, A.R. Williams, Effects of constraint on the oscillatory pattern of endosonic files, J. Endod. 15 (1989) 189–194.
[24] L.M. Jiang, B. Verhaagen, M. Versluis, L.W.M. Van der Sluis, Evaluation of a sonic device designed to activate irrigant in the root canal, J. Endod. 36 (2010) 143–146.
[25] L.W.M. Van der Sluis, M.P. Vogels, B. Verhaagen, R. Macedo, P.R. Wesselink, Study on the influence of refreshment/activation cycles and irrigants on mechanical cleaning efficiency during ultrasonic activation of the irrigant, J. Endod. 36 (2010) 737–740.
[26] B. Verhaagen, C. Boutsioukis, L.W.M. Van der Sluis, M. Versluis, Acoustic streaming induced by an ultrasonically oscillating endodontic file, J. Acoust. Soc. Am. 135 (2014) 1717–1730.
[27] J.P. Robinson, R.G. Macedo, B. Verhaagen, M. Versluis, P.R. Cooper, L.W.M. Van der Sluis, A.D. Walmsley, Cleaning lateral morphological features of the root canal: the role of streaming and cavitation, Int. Endod. J. 51 (2018) e55–e64.
[28] R.A. Roy, M. Ahmad, L.A. Crum, Physical mechanisms governing the hydrodynamic response of an oscillating ultrasonic file, Int. Endod. J. 27 (1994) 197–207.
[29] A. Al-Jadaa, F. Paqué, T. Attin, M. Zehnder, Acoustic hypochlorite activation in simulated curved canals, J. Endod. 35 (2009) 1408–1411.
[30] S.D. De Groot, B. Verhaagen, M. Versluis, M.K. Wu, P.R. Wesselink, L.W.M. Van Der Sluis, Laser-activated irrigation within root canals: cleaning efficacy and flow visualization, Int. Endod. J. 42 (2009) 1077–1083.
[31] R.J. De Moor, M. Meire, K. Goharkhay, A. Moritz, J. Vanobbergen, Efficacy of ultrasonic versus laser-activated irrigation to remove artificially placed dentin debris plugs, J. Endod. 36 (2010) 1580–1583.
[32] K. Yao, K. Satake, S. Watanabe, A. Ebihara, C. Kobayashi, T. Okiji, Effect of laser energy and tip insertion depth on the pressure generated outside the apical foramen during Er: YAG laser-activated root canal irrigation, Photomed. Laser Surg. 35 (2017) 682–687.
[33] W. Kern, The evolution of silicon wafer cleaning technology, J. Electrochem. Soc. 137 (1990) 1887–1892.

[34] G.W. Gale, A.A. Busnaina, Removal of particulate contaminants using ultrasonics and megasonics: a review, Particul, Sci. Technol. 13 (1995) 197–211.
[35] W. Kim, K. Park, J. Oh, J. Choi, H.-Y. Kim, Visualization and minimization of disruptive bubble behavior in ultrasonic field, Ultrasonics 50 (2010) 798–802.
[36] T.-H. Kim, H.-Y. Kim, Disruptive bubble behaviour leading to microstructure damage in an ultrasonic field, J. Fluid Mech. 750 (2014) 355–371.
[37] T. Yamashita, K. Ando, Low-intensity ultrasound induced cavitation and streaming in oxygen-supersaturated water: Role of cavitation bubbles as physical cleaning agents, Ultrason. Sonochem. 52 (2019) 268–279.
[38] R. Park, M. Choi, E.H. Park, W.-J. Shon, H.-Y. Kim, W. Kim, Comparing cleaning effects of gas and vapor bubbles in ultrasonic fields, Ultrason. Sonochem. 76 (2021), 105618.
[39] W. Kim, T.-H. Kim, J. Choi, H.-Y. Kim, Mechanism of particle removal by megasonic waves, Appl. Phys. Lett. 94 (2009), 081908.
[40] J. Choi, T.-H. Kim, H.-Y. Kim, W. Kim, Ultrasonic washing of textiles, Ultrason. Sonochem. 29 (2016) 563–567.
[41] G.L. Chahine, A. Kapahi, J.-K. Choi, C.-T. Hsiao, Modeling of surface cleaning by cavitation bubble dynamics and collapse, Ultrason. Sonochem. 29 (2016) 528–549.
[42] N. Vyas, K. Manmi, Q. Wang, A.J. Jadhav, M. Barigou, R.L. Sammons, S.A. Kuehne, A.D. Walmsley, Which parameters affect biofilm removal with acoustic cavitation? A review, Ultrasound Med. Biol. 45 (2019) 1044–1055.
[43] K.F. Graff, Power ultrasonic transducers: principles and design, in: J.A. Gallego-Juárez, K.F. Graff (Eds.), Power Ultrasonics, Woodhead Publishing, 2015, pp. 127–158.
[44] F. Reuter, R. Mettin, Mechanisms of single bubble cleaning, Ultrason. Sonochem. 29 (2016) 550–562.
[45] S.W. Schneider, A comparison of canal preparations in straight and curved root canals, Oral Surg. Oral Med. Oral Pathol. 32 (1971) 271–275.
[46] C.M. Sedgley, A. Kishen, L.E.C. de Paz, The Root Canal Biofilm, Springer, 2015.
[47] W.H. Ye, B. Fan, W. Purcell, M.M. Meghil, C.W. Cutler, B.E. Bergeron, J.Z. Ma, F. R. Tay, L.-N. Niu, Anti-biofilm efficacy of root canal irrigants against in-situ Enterococcus faecalis biofilms in root canals, isthmuses and dentinal tubules, J. Dent. 79 (2018) 68–76.
[48] A. Shrestha, A. Kishen, Antibiofilm efficacy of photosensitizer-functionalized bioactive nanoparticles on multispecies biofilm, J. Endod. 40 (2014) 1604–1610.
[49] T. Leighton, The acoustic bubble, Academic press, 2012.
[50] B. Verhaagen, S.C. Lea, G.J. De Bruin, L.W.M. Van Der Sluis, A.D. Walmsley, M. Versluis, Oscillation characteristics of endodontic files: numerical model and its validation, IEEE Trans. Ultrason. Ferroelectr. Freq. Control 59 (2012) 2448–2459.
[51] M.S. Plesset, A. Prosperetti, Bubble dynamics and cavitation, Annu. Rev. Fluid Mech. 9 (1977) 145–185.
[52] K. Namura, S. Okai, S. Kumar, K. Nakajima, M. Suzuki, Self-oscillation of locally heated water vapor microbubbles in degassed water, Adv. Mater. Interfaces 7 (2020) 2000483.
[53] M. Strasberg, Onset of ultrasonic cavitation in tap water, J. Acoust. Soc. Am. 31 (1959) 163–176.
[54] N. Gondrexon, V. Renaudin, P. Boldo, Y. Gonthier, A. Bernis, C. Pettier, Degassing effect and gas liquid transfer in a high frequency sonochemical reactor, Chem. Eng. J. 66 (1997) 21–26.
[55] C.E. Brennen, Cavitation and bubble dynamics, Oxford University Press, 1995.
[56] M. Ahmad, T.R.P. Ford, L.A. Crum, Ultrasonic debridement of root canals: an insight into the mechanisms involved, J. Endod. 13 (1987) 93–101.
[57] R. Macedo, B. Verhaagen, D.F. Rivas, M. Versluis, P. Wesselink, L.W.M. Van der Sluis, Cavitation measurement during sonic and ultrasonic activated irrigation, J. Endod. 40 (2014) 580–583.
[58] Z. Ram, Effectiveness of root canal irrigation, Oral Surg. Oral Med. Oral Pathol. 44 (1977) 306–312.
[59] C.O. Lima, A.F.A. Barbosa, C.M. Ferreira, C.M. Augusto, L.M. Sassone, R.T. Lopes, S.R. Fidel, E.J.N.L. Silva, The impact of minimally invasive root canal preparation strategies on the ability to shape root canals of mandibular molars, Int. Endod. J. 53 (2020) 1680–1688.
[60] S.M. Saber, D.M. Hayaty, N.N. Nawar, H.C. Kim, The effect of access cavity designs and sizes of root canal preparations on the biomechanical behavior of an endodontically treated mandibular first molar: a finite element analysis, J. Endod. 46 (2020) 1675–1681.
[61] C. Boutsioukis, Z. Psimma, L.W.M. Van der Sluis, Factors affecting irrigant extrusion during root canal irrigation: a systematic review, Int. Endod. J. 46 (2013) 599–618.
[62] E. Park, Y.A. Shen, M. Haapasalo, Irrigation of the apical root canal, Endod. Topics 27 (2012) 54–73.
[63] E. Park, Y. Shen, M. Khakpour, M. Haapasalo, Apical pressure and extent of irrigant flow beyond the needle tip during positive-pressure irrigation in an in vitro root canal model, J. Endod. 39 (2013) 511–515.
[64] Y. Gao, M. Haapasalo, Y. Shen, H. Wu, B. Li, N.D. Ruse, X. Zhou, Development and validation of a three-dimensional computational fluid dynamics model of root canal irrigation, J. Endod. 35 (2009) 1282–1287.
[65] Z. Psimma, C. Boutsioukis, E. Kastrinakis, L. Vasiliadis, Effect of needle insertion depth and root canal curvature on irrigant extrusion *ex vivo*, J. Endod. 39 (2013) 521–524.
[66] C. Boutsioukis, Z. Psimma, E. Kastrinakis, The effect of flow rate and agitation technique on irrigant extrusion *ex vivo*, Int. Endod. J. 47 (2014) 487–496.
[67] G. Mazue, R. Viennet, J.-Y. Hihn, L. Carpentier, P. Devidal, I. Albaïna, Large-scale ultrasonic cleaning system: design of a multi-transducer device for boat cleaning (20 kHz), Ultrason. Sonochem. 18 (2011) 895–900.
[68] H. Lais, P.S. Lowe, T.H. Gan, L.C. Wrobel, Numerical modelling of acoustic pressure fields to optimize the ultrasonic cleaning technique for cylinders, Ultrason. Sonochem. 45 (2018) 7–16.